

Adsorption of Chlorinated Volatile Organic Compounds in a Fixed Bed of Activated Carbon

Seung Jai Kim[†], Sung Yong Cho and Tae Young Kim

Department of Environmental Engineering, Chonnam National University, Gwangju 500-757, Korea

(Received 19 June 2001 • accepted 28 August 2001)

Abstract—Adsorption isotherms of dichloromethane and 1,1,2-trichloro-1,2,2-trifluoroethane on an activated carbon pellet, Norit B4, were studied. For these chemicals, the Sips equation gave the best fit for the single component adsorption isotherm. The adsorption affinity on activated carbon was greater for dichloromethane than that of 1,1,2-trichloro-1,2,2-trifluoroethane. An experimental and theoretical study was made for the adsorption of dichloromethane and 1,1,2-trichloro-1,2,2-trifluoroethane in a fixed bed. Experimental results were used to examine the effect of operation variables, such as feed concentration, flow rate and bed height. Intraparticle diffusion was able to be explained by a surface diffusion mechanism. An adsorption model based on the linear driving force approximation (LDFA) was found to be applicable to fit the experimental data.

Key words: Adsorption, Dichloromethane, 1,1,2-trichloro-1,2,2-trifluoroethane, Fixed Bed

INTRODUCTION

In recent years, the adsorption process of removing and recovering organic solvents in trace levels from air has attracted special interest as a means of protecting the environment from air pollution. Volatile organic compounds (VOCs) are a family of carbon-containing compounds which are emitted or evaporated into the atmosphere where they participate in photochemical reactions [Jang et al., 1998]. Some VOCs are toxic and carcinogenic. Most VOCs, to varying degrees, contribute to the formation of ground level ozone. The VOCs which may cause stratospheric ozone depletion are mostly a chlorine-containing group of compounds known as chlorofluorocarbons or CFCs. They release chlorine and other halogens into the stratosphere gradually [Wolf, 1992; Cicerone et al., 1974; Cho and Choi, 1996]. These compounds are particularly effective in destroying the ozone even when present in small quantities. VOCs are used as solvents in manufacturing of countless products. Some prominent examples of these products include crystallized organic chemicals, printed materials, paints and coatings and dry-cleaning agents in magnetic tape and semiconductor manufacturing facilities. One consequence of these manufacturing operations is that large amounts of organics are being emitted to the atmosphere. VOCs have been implicated as a major contribution to photochemical smog, which can cause haze, damage plant and animal life, and lead to eye irritation and respiratory problems [Ogura et al., 1992]. Several technologies can be used for recovering VOCs from gaseous wastes, but one of the most important and effective methods for controlling the emission of VOCs is the adsorption process. Temperature swing adsorption using an activated carbon bed is probably the most common adsorption cyclic process for the separation of strongly adsorbed species. It has been widely used in industries for removal and recovery of hydrocarbon and solvent vapors [Chihara et al., 2000]. In this work, the removal of 1,1,2-trichloro-1,2,2-trifluoro-

ethane (CFC-113) and dichloromethane (DCM) was studied theoretically and experimentally.

MATHEMATICAL MODEL

A mathematical model was developed that takes into account the non-ideality of adsorbable species in the adsorbed phase under equilibrium. Applying the typical assumptions [Hwang, 1994] and taking the mass balance of the gas phase in a packed bed, the following governing equation for isothermal adsorption is obtained:

$$\frac{\partial c_i}{\partial t} = D_L \frac{\partial^2 c_i}{\partial z^2} - v \frac{\partial c_i}{\partial z} - \frac{1-\varepsilon}{\varepsilon} \rho_p \frac{\partial q_i}{\partial t} \quad (1)$$

In Eq. (1), the gas-solid mass transfer rate can be expressed as the following linear driving force (LDF) model for surface diffusion [Tien, 1994; Lee and Moon, 2001]:

$$\frac{\partial q_i}{\partial t} = k_s (q_i^* - q_i) = \frac{3k_s}{r_p \rho_p} (c_i - c_i^*) \quad (2)$$

where

$$k_s = \frac{15D_s}{r_p^2} \quad (3)$$

As denoted by Eqs. (2) and (3), the LDF model is an approximation to the solution of Fickian diffusion inside a spherical particle. The expression assumes that the mass transfer rate of adsorption is proportional to the difference between the equilibrium concentration and the bulk concentration of the component. Since the solution of the LDF model is much simpler than the solution of a diffusion model, we employed this model in the present study. By introducing appropriate dimensionless variables, Eq. (1) can be written as follows:

$$\frac{\partial \zeta}{\partial \tau} = \frac{1}{\beta} \frac{\partial^2 \zeta}{\partial S^2} - \frac{\partial \zeta}{\partial S} + \alpha_s (\zeta - \zeta^*) \quad (4)$$

and the dimensionless variables are defined as follows:

[†]To whom correspondence should be addressed.

E-mail: sjkim@chonnam.chonnam.ac.kr

$$\zeta = \frac{c_i}{c_{i0}}, \tau = \frac{vt}{L}, S = \frac{Z}{L}, \beta = \frac{vL}{D_L}, \alpha = \frac{3k_L}{r_p v} \left[\frac{1-\varepsilon}{\varepsilon} \right]$$

The associated initial conditions for $0 < z < L$ is

$$\zeta(z, 0) = 0$$

and the boundary conditions at $z=0$ and $z=L$ for $t>0$ are:

$$\frac{1}{\beta} \frac{\partial \zeta}{\partial S} \Big|_{z=0} = -(\zeta|_{z=0} - \zeta|_{z=0+}) \quad (5)$$

$$\frac{\partial \zeta}{\partial S} \Big|_{z=L} = 0 \quad (6)$$

As previous researchers [Moon and Tien, 1987; Tien, 1994; Wang and Tien, 1982] pointed out in their work on fixed-bed adsorption, if the intraparticle diffusion is described by a homogeneous diffusion model or a lumped parameter model (such as the LDF model), one needs to calculate the concentrations in both phases at the same time. From Eq. (2), the following dynamic condition could be obtained:

$$c_i' + A_i q_i' = B_i \quad (7)$$

where

$$A_i = \frac{r_p \rho_p k_i}{3k_y} \quad \text{and} \quad B_i = c_i + A_i q_i \quad (8)$$

EXPERIMENTAL

The adsorption system in this study consisted of the activated carbon (Norit B4, pellet type), and CFC-113 and DCM. The physical properties of the activated carbon and bed characteristics are given in Tables 1 and 2, respectively. A schematic diagram of the fixed bed experimental setup is presented in Fig. 1. The apparatus was constructed with stainless steel tubes. The adsorption column line is 0.42 cm ID and all other lines are 1/4" ID. Pure nitrogen gas was sent to the solvent saturator. A constant temperature circulator

Table 1. Physical properties of activated carbon

Activated carbon	
Supplier	Norit (B4)
Pellet diameter (mm)	3.9
Pellet length (mm)	6.7
BET surface area (m^2/g)*	826
Micropore fraction (<1 nm)**	45.16%
Porosity	0.42

* from manufacturer

** from nitrogen adsorption at 77 K

Table 2. Experimental conditions for a fixed bed adsorption

Variables	Unit	Range
Bed length	m	0.15-0.25
Flow rate	m/s	$0.369 \cdot 10^{-2}$ - $0.890 \cdot 10^{-2}$
Bed porosity	-	0.12
Packing density	kg/m ³	693.5
Bath temperature	K	298.15-308.15

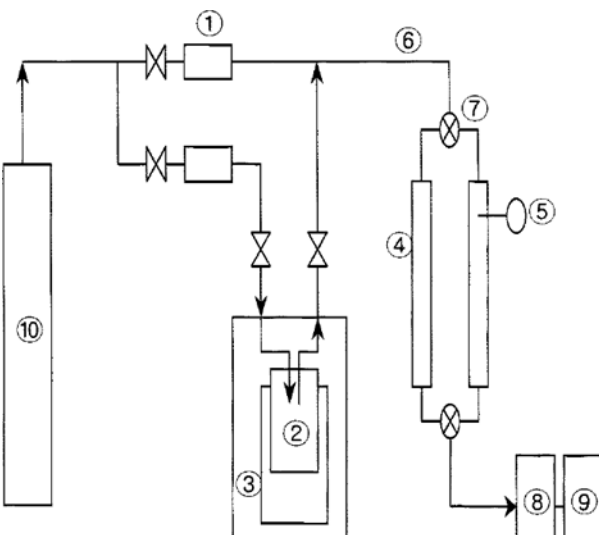


Fig. 1. Flow diagram of adsorption system.

1. Flow meter	6. Heating band
2. Pressure bottle	7. 3 Way valve
3. Water bath	8. G.C.
4. Column	9. P.C.
5. Thermo couple	10. N ₂

(Jeio Tech.) was attached to the pressure bottle in order to keep the temperature constant. The concentrations of solvents were determined from their saturated vapor pressures by assuming vapor-liquid equilibrium state. In order to increase the mixing efficiency of solvents, 6 mm glass beads were packed in the pressure bottle. The gas mixture of the saturated solvent vapor and the pure nitrogen gas was delivered to the adsorption section. The gas flow to the column was controlled by a flow meter that was precalibrated under the experimental pressure conditions. The gas mixture was heated to the experimental temperature in the preheating coil section before being charged to the fixed bed adsorber. The adsorber was made of a stainless steel tube in 1.03 cm ID. A K-type thermocouple was installed at inlet section of the packed column, and the temperature of the system was monitored continuously on a display recorder. The composition of the exit gas stream from the adsorption section was measured in the analyzer section. For this purpose, a gas chromatograph, GC-14B model (Shimadzu), equipped with a hydrogen flame ionization detector was used.

RESULTS AND DISCUSSION

1. Adsorption Equilibrium

The gravimetric method is a well established technique for obtaining adsorption equilibria of pure gases and vapors. 0.1 g of activated carbon in the quartz basket is ventilated to remove impurities within the activated carbon at 503 K for approximately 4 hr by using a vacuum pump. Adsorption amounts are measured at different temperatures of 303 K, 318 K, and 333 K. The adsorbent used for this experiment is Norbit B4 and the adsorbates are CFC-113 and DCM. The adsorption data were obtained by using a high-pressure microbalance. Isotherms of CFC-113 and DCM on the activated carbon at three different temperatures are shown in Figs. 2 and 3, respectively. The isotherms of CFC-113 and DCM were fa-

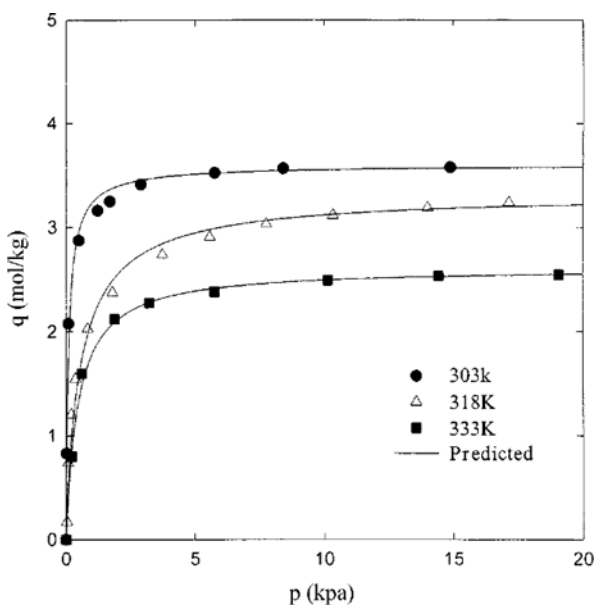


Fig. 2. Adsorption equilibrium curves of $\text{Cl}_2\text{FCCCIF}_2$ on Norit B4 for different temperatures.

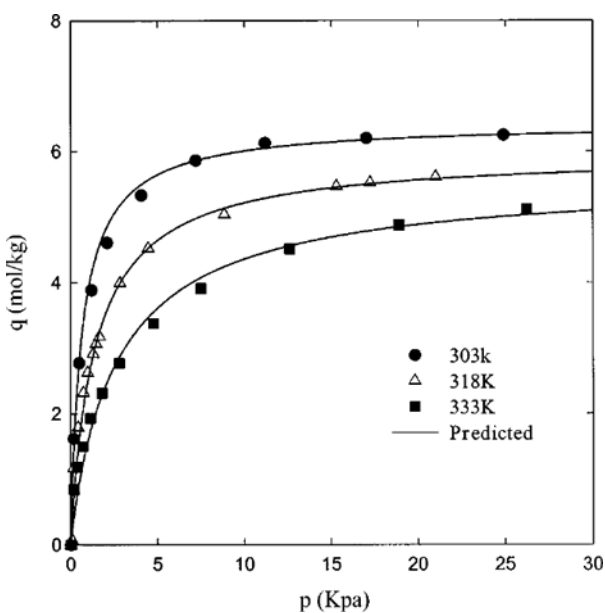


Fig. 3. Adsorption equilibrium curves of CH_2Cl_2 on Norit B4 for different temperatures.

vable types. Single-species isotherm data were correlated by the well-known Langmuir, Freundlich and Sips equations. The parameters of each isotherm were obtained by the least square fitting with experimental data. These parameters and the average percent differences between the measured and calculated values are given in Tables 3 and 4, respectively. Among these isotherms, the Sips equation with three parameters is more appropriate in predicting our data compared to the Langmuir or Freundlich isotherms with two parameters. Isotherms provide information on the affinity of the adsorbent toward the adsorbate as well as the heat of adsorption. The adsorption amounts increase linearly up to a pressure of 0.5 kPa. In

Table 3. Adsorption equilibrium isotherm parameters of Cl_2FC - CCl_2F on activated carbon

Temp. [K]	Langmuir		Freundlich		Sips		
	q_m	b	k	n	q_m	b	n
303	3.48	5.76	2.64	5.18	3.60	8.79	1.13
Error (%)	3.4		17.9		3.8		
318	3.12	2.59	2.04	5.42	3.33	1.75	1.09
Error (%)	3.8		4.3		3.2		
333	2.69	1.89	1.51	4.38	2.6	2.17	1.01
Error (%)	3.3		4.55		2.5		

Table 4. Adsorption equilibrium isotherm parameters of CH_2Cl_2 on activated carbon

Temp. [K]	Langmuir		Freundlich		Sips		
	q_m	b	k	n	q_m	b	n
303	5.91	2.15	3.25	3.83	6.44	1.51	1.03
Error (%)	5.9		11.7		3.5		
318	5.83	0.78	2.76	3.96	5.96	0.73	1.01
Error (%)	1.8		2.8		1.4		
333	5.03	0.51	1.96	3.16	5.60	0.39	1.04
Error (%)	5.1		4.1		3.4		

this pressure range, the affinity of the adsorbate toward the adsorbent is characterized by a Henry's constant. The heats of adsorption can be calculated from the Van't Hoff equation, which is defined as:

$$\ln\left(\frac{p_1}{p_2}\right) = -\frac{\Delta H_a}{R}\left(\frac{1}{T_1} - \frac{1}{T_2}\right) \quad (11)$$

In the Henry law region ($C_\mu = K_p P$), Eq. (11) can be replaced by Eq. (12).

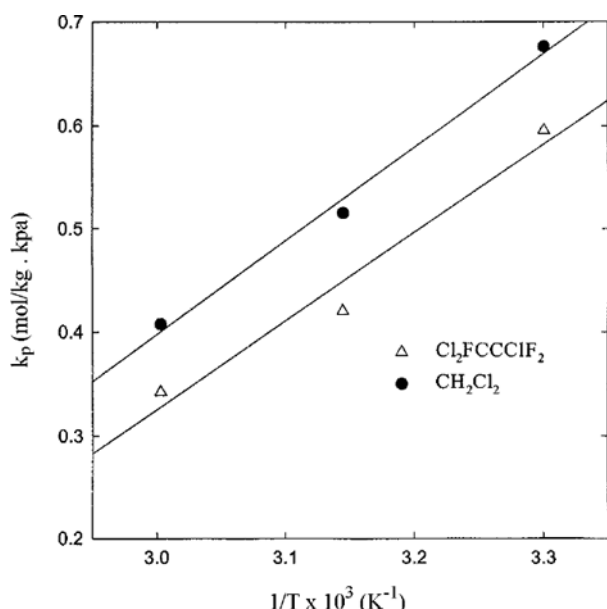


Fig. 4. Temperature dependence of Henry's constant.

$$\ln\left(\frac{k_{p1}}{k_{p2}}\right) = -\frac{\Delta H_2}{R}\left(\frac{1}{T_1} - \frac{1}{T_2}\right) \quad (12)$$

It can be seen from Fig. 4 that the Henry's constant for DCM is greater than that of CFC-113, and DCM is more strongly adsorbed on the activated carbon than CFC-113. The heats of adsorption are almost comparable, although that for DCM (5.9 kcal/mol) is slightly greater than that for CFC-113 (5.0 kcal/mol).

2. Bed Adsorption

A column adsorber has been used as commercial equipment for separation by adsorption since it gives a sharp breakthrough due to the difference in affinity between gases and particles [Park et al., 2001; Hu et al., 2001; Na et al., 2001]. The breakthrough curves of all species, in general, depend on adsorption equilibrium, intraparticle mass transfer, and hydrodynamic conditions in the column. Therefore, it is reasonable to consider adsorption equilibrium and mass transfer simultaneously in simulating the adsorption behavior in the fixed bed adsorber. The operational factors such as input concentration, flow rate and L/D ratio are important in an adsorber designing and optimization. In this work, breakthrough curves were obtained under various experimental conditions mentioned above. The experimental conditions are summarized in Table 2. Fig. 5 shows the effect of film mass transfer coefficient, k_f , on the breakthrough curve of CFC-113. As the value of the mass transfer coefficient increases, the breakthrough curve becomes sharper and the breakthrough behavior is very sensitive to k_f value. This implies that the adsorption equilibrium controls the breakthrough as the mass transfer resistance dwindles. k_f for CFC-113 is approximately 10^{-3} m/s. The breakthrough curves of CFC-113 and DCM at the same conditions are shown in Fig. 6. The breakthrough time of CFC-113 is shorter than DCM because the affinity of CFC-113 is smaller than that for DCM. This figure also shows that the predicted breakthrough curves by the LDFA model incorporated with the Sips equation are fitted well with the fixed bed data for single component systems. Fig. 7 shows the effect of bed height on the CFC-113 adsorption.

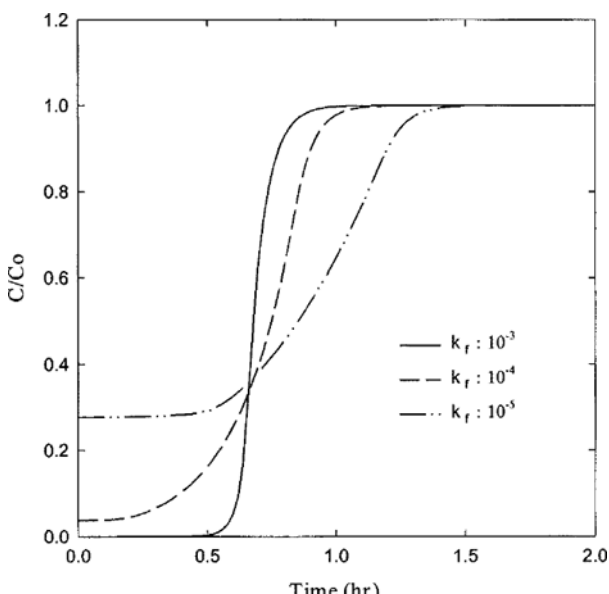


Fig. 5. Effect of k_f on single-specie breakthrough curves of $\text{Cl}_2\text{-FCCCClF}_2$.

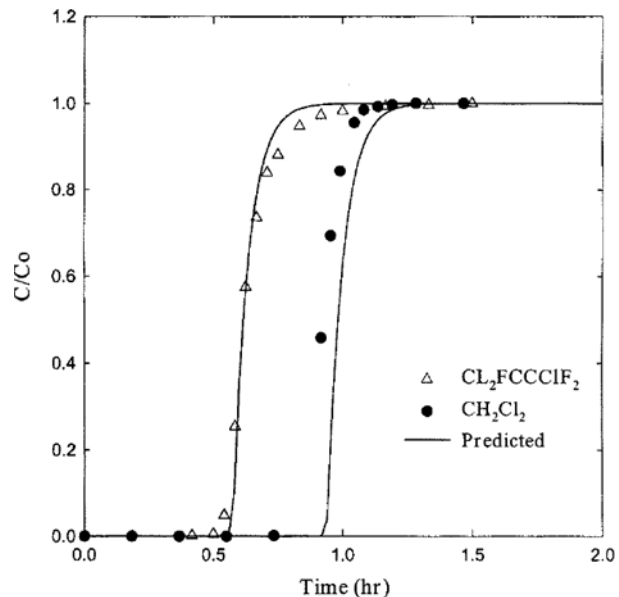


Fig. 6. Comparison of breakthrough curves of $\text{Cl}_2\text{FCCCClF}_2$ and CH_2Cl_2 adsorption on Norit B4 (25 °C, L: 0.15 m, v: 0.369×10^{-2} m/s).

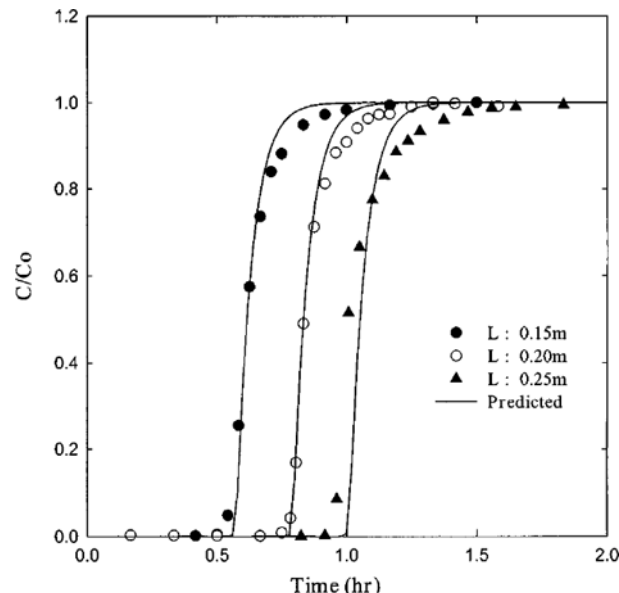


Fig. 7. Experimental and predicted breakthrough curves of $\text{Cl}_2\text{FCCCClF}_2$ adsorption for different bed heights (25 °C, v: 0.369×10^{-2} m/s).

The breakthrough curves for different bed heights are similar in shape. Since the breakthrough curve retains a constant pattern, it may be interpreted that the adsorption zone has a constant length.

The effect of flow rate on adsorption was studied and the results are shown in Fig. 8. This figure shows that the breakthrough time decreased with increasing flow rate, and the breakthrough curves are slightly steeper for higher flow rates. These trends are consistent with general behavior of a fixed bed adsorber. Since the intraparticle diffusivity is usually independent of flow rate, this behavior is due to the external film mass transfer resistance. This resis-

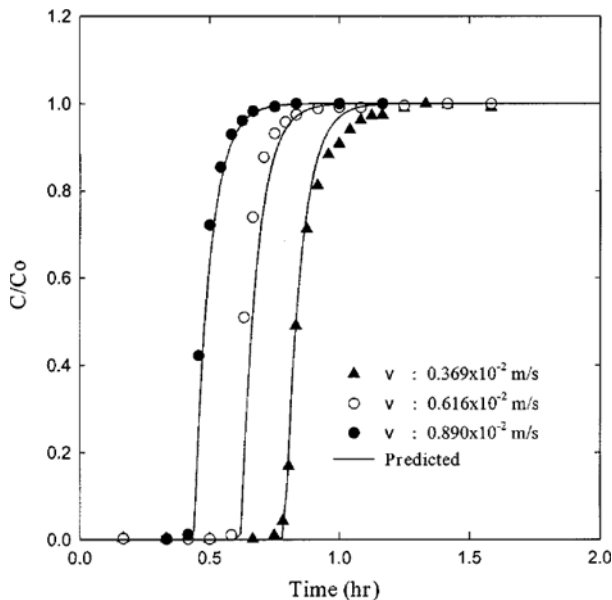


Fig. 8. Experimental and predicted breakthrough curves of $\text{Cl}_2\text{-FCCCl}_2$ adsorption for different flow rates (25 °C, L: 0.2 m).

tance decreased with the flow rate, so that the length of the mass transfer zone is reduced, and a sharper breakthrough curve is generated. In modeling for a packed bed adsorber, the main parameters concerning the transport of adsorbates are the axial dispersion coefficient and the external film mass transfer coefficient [Row and Choi, 1990; Markovska et al., 2001]. Usually, the axial dispersion coefficient comes from the contribution of molecular diffusion and turbulent mixing arising from the spilling and recombination of flows around the adsorbent particle. In this study, the axial dispersion coefficient, D_L , was calculated from the following correlation given by Edwards and Richardson [1968].

$$\frac{1}{Pe} = \frac{r_i \epsilon_B}{Re Sc} + \frac{1}{Pe'_c \left[1 + \frac{\beta r_i \epsilon_B}{Re Sc} \right]} \quad (13)$$

The constant values for this calculation are

$$r_i = 0.73, \beta = 13.0, Pe'_c = 2.0$$

The film mass transfer coefficient, k_f , in a fixed bed adsorber is obtained by Wakao and Funazkri [1978]:

$$Sh = \frac{2k_f R_p}{D_m} = 2.0 + 1.1 Sc^{1/3} Re^{0.6} \quad (14)$$

where, D_m is molecular diffusivity, Sh is Sherwood number, Sc and

Table 5. Mass transfer parameters for a fixed bed model simulation

Parameters	Symbols (unit)	$\text{Cl}_2\text{-FCCCl}_2$	CH_2Cl_2
Axial dispersion coefficient	$D_L (\text{m}^2/\text{s})$	$4.20 \cdot 10^{-5}$	$4.43 \cdot 10^{-5}$
Film mass transfer coefficient	$k_f (\text{m/s})$	$1.56 \cdot 10^{-3}$	$2.10 \cdot 10^{-3}$
Surface diffusivity	$D_s (\text{m}^2/\text{s})$	$1.10 \cdot 10^{-9}$	$1.50 \cdot 10^{-9}$
Molecular diffusivity	$D_m (\text{m}^2/\text{s})$	$1.15 \cdot 10^{-5}$	$1.56 \cdot 10^{-5}$

R_e are Schmidt and Reynolds numbers, respectively. Molecular diffusion coefficients, D_m , for CFC-113 and DCM are obtained by Fuller et al. [1969]. Under the experimental conditions of this study, the estimated values of axial dispersion coefficient and external film mass transfer coefficient, and molecular diffusion in the fixed bed are listed in Table 5.

Fig. 9 shows the effect of the flow rate on the adsorption of DCM in the fixed bed. As shown in this figure, the effluent concentration increases with the flow rate. This is due to the fact that at a higher flow rate, the contact time between the adsorbent and the gas phase in the bed is shorter. Fig. 10 illustrates the effect of inlet concentration

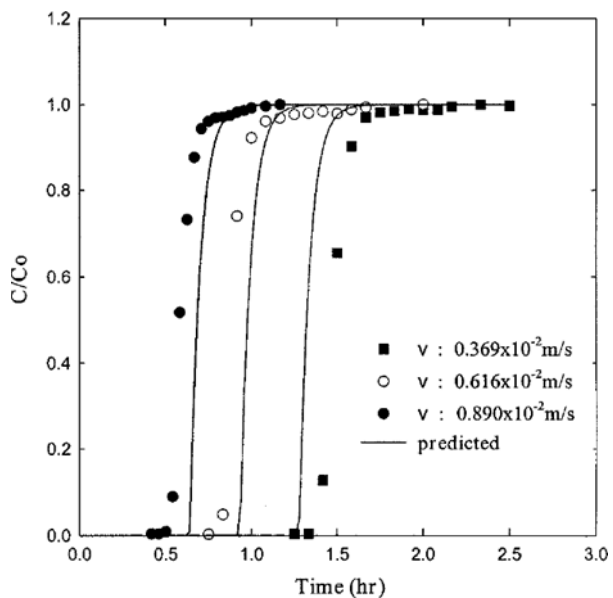


Fig. 9. Experimental and predicted breakthrough curves of CH_2Cl_2 adsorption for different flow rates (25 °C, L: 0.2 m).

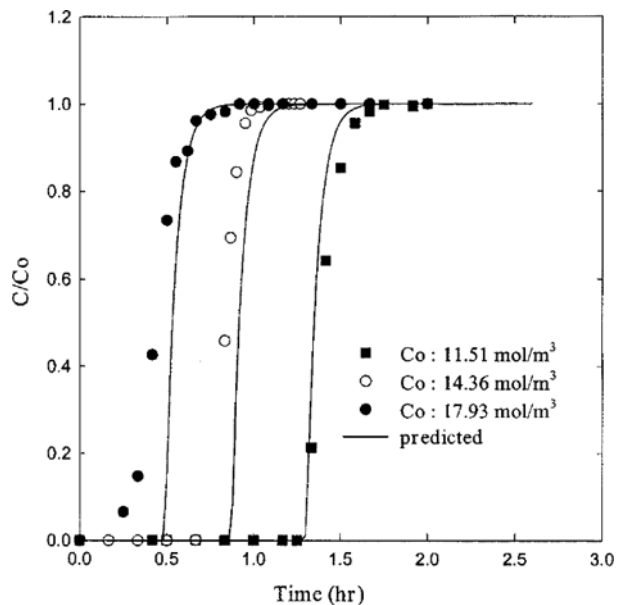


Fig. 10. Experimental and predicted breakthrough curves of CH_2Cl_2 adsorption for different inlet concentrations (L: 0.15 m, v: $0.369 \times 10^{-2} \text{ m/s}$).

on experimental breakthrough curves for DCM. The breakthrough time decreases with the increase of inlet concentration. The result can be explained by the concept of the mass transfer zone (MTZ) velocity [Ruthven, 1984]. The velocity of MTZ is a function of interstitial velocity, particle density, bed porosity, and the slope of the equilibrium isotherm. For a linear isotherm adsorption system, the velocity of MTZ is constant. Therefore the breakthrough time is not affected by inlet concentrations at constant MTZ velocity. However, the adsorption isotherm of CFC-113 on activated carbon is favorable as shown in Fig. 2. As the inlet concentration increases, the value of slope of the equilibrium isotherm decreases and the MTZ velocity increases. Therefore, the breakthrough time becomes shorter under this circumstance.

CONCLUSIONS

Adsorption capacities of solvent vapors such as 1,1,2-trichloro-1,2,2-trifluoroethane and dichloromethane on an activated carbon pellet (Norit B4) were measured experimentally at various temperatures. Single-species equilibrium data show typical type II isotherms. The Sips equation gave the best fit for the single-component adsorption of 1,1,2-trichloro-1,2,2-trifluoroethane and dichloromethane on activated carbon. The adsorption affinity on activated carbon was greater for dichloromethane than that of 1,1,2-trichloro-1,2,2-trifluoroethane. Adsorption behavior in the fixed-bed was studied in terms of flow rates, heights of the bed, and concentrations of the adsorbates. The adsorption processes of 1,1,2-trichloro-1,2,2-trifluoroethane and dichloromethane vapors on activated carbon were found to be controlled by intraparticle mass transfer, and surface diffusion was a dominant intraparticle mass transfer mechanism. Adsorption dynamics of 1,1,2-trichloro-1,2,2-trifluoroethane and dichloromethane in the fixed-bed can be simulated by the LDFA (Linear Driving Force Approximation).

ACKNOWLEDGEMENT

This research was financially supported by the Korea Science and Engineering Foundation (No. 98-1111-2066-2).

NOMENCLATURE

A_i	: dynamic condition of component i
B_i	: dynamic condition of component i
c_i	: bulk phase concentration of component i [mol/m ³]
c_i^*	: equilibrium concentration of component i [mol/m ³]
c_a	: adsorbed concentration on solid phase [mol/m ³]
D_L	: axial dispersion coefficient [m/s]
D_s	: surface diffusion coefficient [m ² /s]
k_f	: film mass transfer coefficient [m/s]
k_p	: Henry's constant [mol/kg kpa]
k_s	: LDF mass transfer coefficient [1/s]
L	: bed length [m]
p	: pressure [kpa]
P_e	: Peclet number
q_i	: adsorbed amount of component i at equilibrium [mol/kg]
q_i^*	: adsorbed amount of component i at pure state [mol/kg]
r_p	: particle radius [m]

S	: dimensionless axial distance
t	: time [hr]
T	: temperature [K]
v	: superficial velocity [m/s]
z	: axial distance coordinate [m]

Greek Letters

α	: dimensionless variable [-]
β	: dimensionless [-]
ε	: bed void fraction [-]
ζ	: dimensionless concentration [-]
ρ_p	: particle density [kg/m ³]
τ	: dimensionless time [-]

REFERENCES

Chihara, K., Mellot, C. F., Cheetham, A. K., Harms, S., Mangyo, H., Omote, M. and Kamiyama, R., "Molecular Simulation for Adsorption of Chlorinated Hydrocarbon in Zeolites," *Korean J. Chem. Eng.*, **17**, 649 (2001).

Cho, S. Y. and Choi, D. K., "Langmuir Parameters for Adsorption of Two Halogenated Chemicals on an Activated Carbon Pellet," *Korean J. Chem. Eng.*, **13**, 409 (1996).

Cicerone, R. J., Stolarski, R. S. and Walters, S., "Stratospheric Ozone Destruction by Man Made Chlorofluoromethanes," *Science*, **185**, 1165 (1974).

Edwards, M. F. and Richardson, J. F., "Gas Dispersion in Parked Beds," *Chem. Eng. Sci.*, **23**, 109 (1968).

Hu, H. B., Yao, S. J., Zhu, Z. Q. and Hur, B. K., "Comparison of the Adsorption Characteristics of Expanded Bed Adsorbent with Conventional Chromatographic Adsorbent," *Korean J. Chem. Eng.*, **18**, 357 (2001).

Hwang, K. S., "Separation of H₂/CO₂, H₂/CO Gas Mixtures by Pressure Swing Adsorption and Fixed-Bed Dynamics," Ph.D dissertation, KAIST (1994).

Jang, B. H., Lee, S. S., Yeon, T. H. and Tie, T. E., "Effects of Base Metal Promoters in VOC Catalysts for Chlorocarbons and n-Hexane Oxidation," *Korean J. Chem. Eng.*, **15**, 516 (2001).

Lee, D. H. and Moon, H., "Adsorption Equilibrium of Heavy Metals on Natural Zeolites," *Korean J. Chem. Eng.*, **18**, 625 (2001).

Markowska, L., Meshko, V. and Noveski, V., "Adsorption of Basic Dyes in a Fixed Bed Column," *Korean J. Chem. Eng.*, **18**, 190 (2001).

Moon, H. and Tein, C., "Further Work on Multicomponent Adsorption Equilibria Calculations Based on the Ideal Adsorbed Solution Theory," *Ind. Eng. Chem. Res.*, **26**, 2042 (1987).

Na, B. K., Koo, K. K., Eum, H. M., Lee, H. and Song, H. K., "CO₂ Recovery from Flue Gas by PSA Process using Activated Carbon," *Korean J. Chem. Eng.*, **18**, 220 (2001).

Ogura, K., Kobayashi, W., Migita, C. T. and Kakum, K., "Complete Photodecomposition of CFC-113, CHCl₃ and CCl₄ and Scavenging of Generated Reactive Species," *Environ. Technol.*, **13**, 81 (1992).

Park, I. S., Kwak, C. and Hwang, Y. G., "Frequency Response of Adsorption of a Gas onto Bidisperse Pore-Structured Soil with Modulation of Inlet Molar Flow-Rate," *Korean J. Chem. Eng.*, **18**, 330 (2001).

Row, K. H., Choi, D. K. and Lee, Y. Y., "Simulation of the Combined Continuous and Preparative Separation of Three Close-Boiling Com-

ponents in Gas-Liquid Chromatography," *Korean J. Chem. Eng.*, **7**, 287 (1990).

Ruthven, D. M., "Principles of Adsorption and Adsorption Processes," Wiley, New York, U.S.A. (1995).

Tien, C., "Adsorption Calculations and Modeling," Butterworths-Heinemann (1994).

Wang, S. C. and Tien, C., "Further Work on Multicomponent Liquid Phase Adsorption in Fixed Beds," *AICHE J.*, **28**, 565 (1982).

Wakao, N. and Funazkri, T., "Effect of Fluid Dispersion Coefficient on Particle to Fluid Mass Transfer Coefficients in Packed Bed," *J. of Chem. Sci.*, **33**, 1375 (1978).

Wolf, K., "Ozone Depletion and the use of CFCs," *J. Environ. Sci.*, **32**, 41 (1992).